Article

Differential Line Broadening in MAS Solid-State NMR due to Dynamic Interference

Veniamin Chevelkov, Katja Faelber, Anna Schrey, Kristina Rehbein, Anne Diehl, and Bernd Reif

J. Am. Chem. Soc., **2007**, 129 (33), 10195-10200• DOI: 10.1021/ja072024c • Publication Date (Web): 31 July 2007

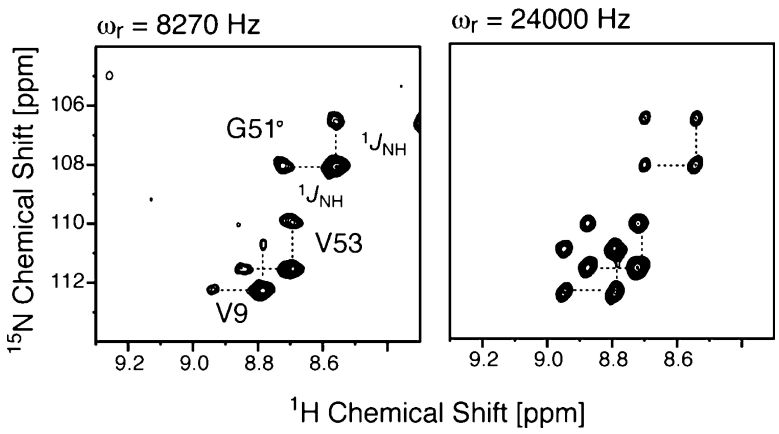

More About This Article

Additional resources and features associated with this article are available within the HTML version:

- Supporting Information
- Links to the 9 articles that cite this article, as of the time of this article download
- Access to high resolution figures
- Links to articles and content related to this article
- Copyright permission to reproduce figures and/or text from this article

View the Full Text HTML

J|A|C|S
ARTICLES
Published on Web 07/31/2007

Differential Line Broadening in MAS Solid-State NMR due to Dynamic Interference

Veniamin Chevelkov,[†] Katja Faelber,[†] Anna Schrey,[†] Kristina Rehbein,[†] Anne Diehl,[†] and Bernd Reif*[,†,‡]

Contribution from the Leibniz-Forschungsinstitut für Molekulare Pharmakologie (FMP), Robert-Rössle-Str. 10, D-13125 Berlin, Germany, and Charité Universitätsmedizin, D-10115 Berlin, Germany

Received March 22, 2007; E-mail: reif@fmp-berlin.de

Abstract: Many MAS (magic angle spinning) solid-state NMR investigations of biologically relevant protein samples are hampered by poor resolution, particularly in the ^{15}N chemical shift dimension. We show that dynamics in the nanosecond−microsecond time scale in solid-state samples can induce significant line broadening of ^{15}N resonances in solid-state NMR experiments. Averaging of $^{15}NH^{\alpha/\beta}$ multiplet components due to ^{1}H decoupling induces effective relaxation of the ^{15}N coherence in case the N−H spin pair undergoes significant motion. High resolution solid-state NMR spectra can then only be recorded by application of TROSY (Transverse Relaxation Optimized Spectroscopy) type techniques which select the narrow component of the multiplet pattern. We speculate that this effect has been the major obstacle to the NMR spectroscopic characterization of many membrane proteins and fibrillar aggregates so far. Only in very favorable cases, where dynamics are either absent or very fast (picosecond), high-resolution spectra were obtained. We expect that this approach which requires intense deuteration will have a significant impact on the quality and the rate at which solid-state NMR spectroscopic investigations will emerge in the future.

Introduction

At present, characterization of dynamic processes in biological macromolecules tends to be a field of solution-state NMR spectroscopy. However, solid-state NMR spectroscopy also holds a great potential for the study of these processes. So far, it is not very well understood why the spectra of a few amyloidogenic peptides or membrane proteins are characterized by very broad resonance lines,[1,2] whereas others display a very favorable spectral quality.[3−6] The assumption that dynamic processes are maybe the origin of these obstructive properties is corroborated by studies which demonstrate that molecules in an amyloid fibril can undergo chemical exchange between an amyloid fibril-type conformation and a soluble molecule.[7,8] Analogous to solution-state NMR spectroscopy, dynamic processes result in averaging of the H^{α}/H^{β} proton spin states in standard ^{1}H decoupled solid-state NMR experiments, with all the detrimental consequences to the spectra that are observed in solution-state NMR for very large proteins. On the other hand, interference between different relaxation mechanisms can be employed to manipulate the relaxation properties of a certain spin. These effects were explored with great success by Wüthrich and co-workers and resulted in the development of the TROSY (Transverse Relaxation Optimized Spectroscopy) technique.[9−13]

Study of dynamic processes in the solid-state attracted much attention recently,[14−17] as the measured experimental parameter (e.g., ^{15}N T_1, ^{2}H quadrupolar coupling) is dependent only on local motional processes and is not coupled to the global reorientation time τ_C of the molecule as in solution-state NMR. In order to investigate exactly how protein dynamics influence the resolution of MAS solid-state NMR spectral line shapes, we performed experiments on a microcrystalline sample of the

[†] Leibniz-Forschungsinstitut für Molekulare Pharmakologie (FMP).
[‡] Charité Universitätsmedizin.

(1) Petkova, A. T.; Ishii, Y.; Balbach, J. J.; Antzutkin, O. N.; Leapman, R. D.; Delaglio, F.; Tycko, R. *Proc. Natl. Acad. Sci. U.S.A.* **2002**, *99* (26), 16742−16747.
(2) Ventura, S.; Zurdo, J.; Narayanan, S.; Parreño, M.; Mangues, R.; Reif, B.; Chiti, F.; Giannoni, E.; Dobson, C. M.; Aviles, F. X.; Serrano, L. *Proc. Natl. Acad. Sci. U.S.A.* **2004**, *101* (19), 7258−7263.
(3) Jaroniec, C. P.; MacPhee, C. E.; Astrof, N. S.; Dobson, C. M.; Griffin, R. G. *Proc. Natl. Acad. Sci. U.S.A.* **2002**, *99* (26), 16748−16753.
(4) Siemer, A. B.; Ritter, C.; Ernst, M.; Riek, R.; Meier, B. H. *Angew. Chem., Int. Ed.* **2005**, *44* (16), 2441−2444.
(5) Heise, H.; Hoyer, W.; Becker, S.; Andronesi, O. C.; Riedel, D.; Baldus, M. *Proc. Natl. Acad. Sci. U.S.A.* **2005**, *102* (44), 15871−15876.
(6) Chevelkov, V.; Chen, Z.; Bermel, W.; Reif, B. *J. Magn. Reson.* **2005**, *172*, 56−62.
(7) Carulla, N.; Caddy, G. L.; Hall, D. R.; Zurdo, J.; Gairi, M.; Feliz, M.; Giralt, E.; Robinson, C. V.; Dobson, C. M. *Nature* **2005**, *436* (7050), 554−558.
(8) Narayanan, S.; Reif, B. *Biochemistry* **2005**, *44* (5), 1444−1452.
(9) Pervushin, K.; Riek, R.; Wider, G.; Wüthrich, K. *Proc. Natl. Acad. Sci. U.S.A.* **1997**, *94*, 12366−12371.
(10) Wider, G.; Wüthrich, K. *Curr. Opin. Struct. Biol.* **1999**, *9* (5), 594−601.
(11) Pervushin, K. *Quart. Rev. Biophys.* **2000**, *33* (2), 161−197.
(12) Riek, R.; Fiaux, J.; Bertelsen, E. B.; Horwich, A. L.; Wuthrich, K. *J. Am. Chem. Soc.* **2002**, *124* (41), 12144−12153.
(13) Fiaux, J.; Bertelsen, E. B.; Horwich, A. L.; Wüthrich, K. *Nature* **2002**, *418*, 207−210.
(14) Giraud, N.; Böckmann, A.; Lesage, A.; Penin, F.; Blackledge, M.; Emsley, L. *J. Am. Chem. Soc.* **2004**, *126* (37), 11422−11423.
(15) Hologne, M.; Chevelkov, V.; Reif, B. *Prog. Nucl. Magn. Reson. Spectrosc.* **2006**, *48*, 211−232.
(16) Reif, B.; Xue, Y.; Agarwal, V.; Pavlova, M. S.; Hologne, M.; Diehl, A.; Ryabov, Y. E.; Skrynnikov, N. R. *J. Am. Chem. Soc.* **2006**, *128* (38), 12354−12355.
(17) Lorieau, J. L.; McDermott, A. E. *J. Am. Chem. Soc.* **2006**, *128* (35), 11505−11512.

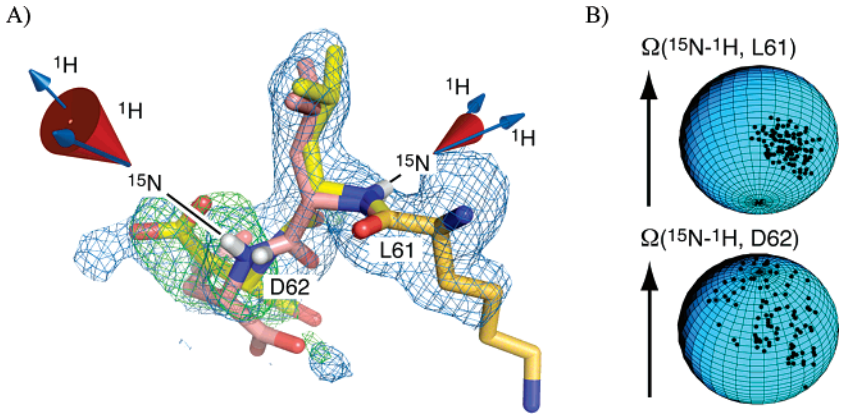

Figure 1. (A) Electron density (1σ 2fofc, blue, 3σ, fofc, green) of the X-ray structure at the C-terminus of the chicken α-spectrin SH3 domain determined at room temperature. The final, deposited structural model (PDB code 2NUZ) contains only L61. D62 is not included in the final structure. The indicated models represent roughly the electron density but are inconsistent with experimental X-ray data (increased R^{free}). Depending on local dynamics, N−H bond vectors (blue arrows) can adopt different orientations within a cone (schematically indicated in red). (B) Distribution of N−H tensor orientations of L61 and D62 represented as spatial angles Ω during a 1 ns molecular dynamics trajectory sampled every 5 ps for the amino acids L61 and D62. Before the analysis of the $^{15}N,^{1}H$ coordinates, the protein was aligned according to its diffusion tensor in order to account for molecular tumbling.

chicken α-spectrin SH3 domain. Figure 1 displays the C-terminal part of the X-ray structural model of this SH3 domain at room temperature together with the respective electron densities for the residues L61 and D62 (PDB code: 2NUZ). The protein crystals diffracted to a maximum resolution of 1.85 Å. The structure could be refined to final *R*-factors of $R^{cryst} = 17.5\%$ and $R^{free} = 18.4\%$, respectively. In the crystal structure, the *B*-factors for C^{α} atoms clearly increased from K59 (29.6 Å^2) to K60 (31.9 Å^2) and L61 (34.3 Å^2). These *B*-factors are significantly higher than the mean *B*-factor of the main chain (26.9 Å^2) indicating an increasing flexibility or disorder toward the end of the peptide chain. The high flexibility of D62 allows for a larger variation of the spatial angle Ω that the N−H bond vector adopts with respect to the external magnetic field (Figure 1B). In this case, the conformational heterogeneities responsible for the increased *B*-factors for D62 arise from dynamics rather than crystal imperfections. Time dependent fluctuations of the local magnetic field induced by variations in the chemical shift anisotropy (CSA) of the nitrogen nucleus and the $^{15}N-^{1}H$ dipole (DD) would result in relaxation of the nitrogen magnetization due to CSA/DD cross correlated relaxation.

Results and Discussion

The above-mentioned hypothesis can be tested on ^{15}N labeled perdeuterated, crystalline protein. Perdeuteration of a protein yields efficient dilution of the proton spin system. Subsequent back-exchange of amide protons reintroduces only weak $^{1}H,^{1}H$ dipolar couplings which are efficiently suppressed by MAS.[18−20] In these experiments, the ^{1}H line width of most of the resonances is typically on the order of 150−250 Hz and 80−150 Hz in the absence and presence of homonuclear decoupling, respectively.[21] We could show recently that ultrahigh resolution ^{1}H spectra are obtained in MAS solid-state NMR if the respective perdeuterated protein is recrystallized from a buffer containing 90% D_2O.[22,23] The resultant ^{1}H line width is on the order of 17−35 Hz for MAS spinning frequencies in the range 8−24 kHz. This approach enables ^{1}H detected 2D $^{1}H,^{15}N$ correlation spectroscopy without homo- and heteronuclear dipolar decoupling. At the same time, $^{1}H,^{15}N$ scalar couplings can be easily resolved in either the direct or indirect evolution period of a multidimensional NMR experiment. Furthermore, this labeling strategy also allows the determination of H^N-H^N long-range distances,[19,24,25] detection of dynamic water molecules,[25,26] and the characterization of side chain dynamics using deuterium.[27,28]

Acquistion of $^{1}H,^{15}N$ correlation spectra without application of heteronuclear scalar decoupling results in TROSY type spectra as represented in Figure 2. Each correlation peak is split into a doublet in both the ^{1}H and ^{15}N dimensions due to evolution of the $^{1}J_{HN}$ scalar coupling. As in TROSY, the intensities of the individual components of the multiplet pattern are not equal. In solution-state NMR, the size of this effect is determined only by the reorientation time τ_C of the molecule in solution. In the case of solid-state NMR, however, two effects come into play: (1) Static interference of the ^{15}N CSA and $^{1}H-^{15}N$ dipolar tensors. Both interactions act simultaneoulsy on the ^{15}N nucleus. (2) Dynamic interference due to $^{15}N/^{1}H-^{15}N$ cross-correlated relaxation. The presence of backbone dynamics in the solid state has been suggested recently by Emsley and coworkers.[14,29−31]

Static interference effects are well documented in solid-state NMR experiments.[32−37] If scalar couplings are resolved in the

(18) McDermott, A. E.; Creuzet, F. J.; Kolbert, A. C.; Griffin, R. G. *J. Magn. Reson.* **1992**, *98*, 408−413.
(19) Reif, B.; Jaroniec, C. P.; Rienstra, C. M.; Hohwy, M.; Griffin, R. G. *J. Magn. Reson.* **2001**, *151* (2), 320−327.
(20) Chevelkov, V.; Rossum, B. J. v.; Castellani, F.; Rehbein, K.; Diehl, A.; Hohwy, M.; Steuernagel, S.; Engelke, F.; Oschkinat, H.; Reif, B. *J. Am. Chem. Soc.* **2003**, *125*, 7788−7789.
(21) Morcombe, C. R.; Paulson, E. K.; Gaponenko, V.; Byrd, R. A.; Zilm, K. W. *J. Biomol. NMR* **2005**, *31* (3), 217−230.
(22) Chevelkov, V.; Rehbein, K.; Diehl, A.; Reif, B. *Angew. Chem., Int. Ed.* **2006**, *45*, 3878−3881.
(23) Agarwal, V.; Diehl, A.; Skrynnikov, N.; Reif, B. *J. Am. Chem. Soc.* **2006**, *128*, 12620−12621.
(24) Reif, B.; van Rossum, B. J.; Castellani, F.; Rehbein, K.; Diehl, A.; Oschkinat, H. *J. Am. Chem. Soc.* **2003**, *125* (6), 1488−1489.
(25) Paulson, E. K.; Morcombe, C. R.; Gaponenko, V.; Dancheck, B.; Byrd, R. A.; Zilm, K. W. *J. Am. Chem. Soc.* **2003**, *125* (47), 14222−14223.
(26) Chevelkov, V.; Faelber, K.; Diehl, A.; Heinemann, U.; Oschkinat, H.; Reif, B. *J. Biomol. NMR* **2005**, *31*, 295−310.
(27) Hologne, M.; Faelber, K.; Diehl, A.; Reif, B. *J. Am. Chem. Soc.* **2005**, *127* (33), 11208−11209.
(28) Hologne, M.; Chen, Z.; Reif, B. *J. Magn. Res.* **2006**, *179* (1), 20−28.
(29) Giraud, N.; Blackledge, M.; Goldman, M.; Böckmann, A.; Lesage, A.; Penin, F.; Emsley, L. *J. Am. Chem. Soc.* **2005**, *127* (51), 18190−18201.
(30) Giraud, N.; Sein, J.; Pintacuda, G.; Böckmann, A.; Lesage, A.; Blackledge, M.; Emsley, L. *J. Am. Chem. Soc.* **2006**, *128*, 12398−12399.
(31) Giraud, N.; Blackledge, M.; Böckmann, A.; Emsley, L. *J. Magn. Reson.* **2007**, *184*, 51−61.
(32) Zilm, K. W.; Grant, D. M. *J. Am. Chem. Soc.* **1981**, *103* (11), 2913−2922.

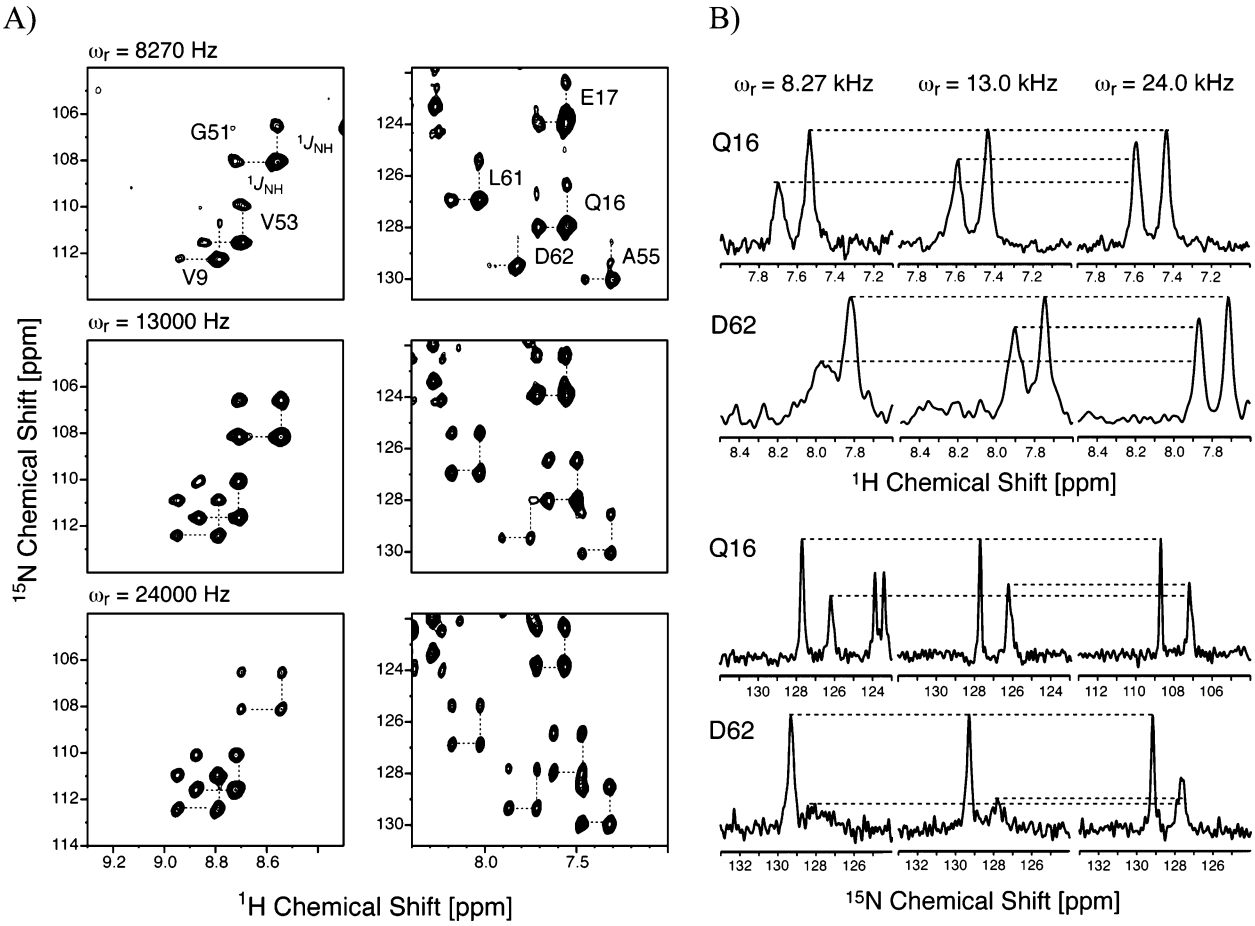

Figure 2. (A) 2D ^{1}H,^{15}N correlation spectra recorded at different MAS rotation frequencies. All spectra were recorded at an external magnetic field strength of 14.1 T (corresponding to a ^{1}H Larmor frequency of 600 MHz). Each signal is split into a doublet due to the $^1J_{NH}$ scalar coupling. (B) 1D traces through selected correlation signals along the ^{1}H (top) and the ^{15}N dimension (bottom).

solid state, the two resonances originating from the H^{α} and H^{β} spin states in the ^{15}N spectrum are associated with different anisotropies: The upfield and downfield components in the nitrogen dimension are related approximately to the sum and difference of the ^{15}N CSA and the ^{15}N−^{1}H dipolar interaction, respectively. As the interaction Hamiltonian of the ^{15}N spin can be considered to be purely inhomogeneous in the sense of Maricq and Waugh,[38] no MAS frequency dependence of the line widths is expected for the case of static interference. The intensities of the $N-H^{\alpha/\beta}$ multiplet components are therefore only dependent on the MAS rotation frequency. This is evident from the finding that, at larger MAS frequencies, the total signal intensity is no longer distributed over multiple rotational spinning side bands. A more thorough consideration is given as part of the Supporting Information in order to outline the physical basis of this effect. It is obvious that variations in the size and orientation of the ^{15}N CSA as well as the ^{15}N−^{1}H dipolar tensor will change the relative $^{15}N-H^{\alpha/\beta}$ multiplet intensity ratio at a given MAS rotation frequency. This effect is, however, negligible assuming the variation of tensor parameters which have been experimentally determined so far (see Supporting Information). In addition to the static effect which is based on the chemical properties of an individual amino acid, only dynamics can then contribute to a differential line width for $N-H^{\alpha/\beta}$ multiplet components.

Static interference effects are usually not observed in solution-state NMR, since they are averaged to zero due to the tumbling of the molecule in solution. However, a second-order dynamic interference effect which is based on dipolar and chemical shift anisotropy relaxation interference still influences the spectra. This effect is the physical basis of TROSY[9] and cross-correlated relaxation experiments.[39,40] The size of the ^{15}N CSA,^{15}N−^{1}H dipole cross-correlated relaxation rate can be expressed as[39]

$$\Gamma^{\mathrm{CSA/DD}} = 2\alpha\, d\{4J(0) + 3J(\omega_N)\}\, P_2(\cos\theta) \qquad (1)$$

where $\alpha = -4\pi/3B_0(\sigma_{||} - \sigma_{\perp})r_{\mathrm{HN}}{}^3/(h\gamma_{\mathrm{H}})$, and $d = \gamma_{\mathrm{H}}{}^2\gamma_{\mathrm{N}}{}^2h^2/(80\pi^2 r_{\mathrm{HN}}{}^6)$. r_{HN} refers to the H−N bond length. P_2 refers to the second order Legendre polynomial $^1/_2(3\cos^2\theta - 1)$ with θ corresponding to the angle between the principal axis of the N−H dipolar vector and the ^{15}N CSA shielding tensor. Experiments have shown that θ adopts values on the order of 20°−24°.[41,42] For an isotropic motional model without internal

(33) Harris, R. K.; Packer, K. J.; Thayer, A. M. *J. Magn. Res.* **1985**, *62*, 284−297.
(34) Griffey, D.; Redfield, A. *Quart. Rev. Biophys.* **1987**, *19*, 51−82.
(35) Wu, G.; Sun, B.; Wasylishen, R. E.; Griffin, R. G. *J. Magn. Reson.* **1997**, *124*, 366−371.
(36) Duma, L.; Hediger, S.; Lesage, A.; Sakellariou, D.; Emsley, L. *J. Magn. Res.* **2003**, *162*, 90−101.
(37) Igumenova, T. I.; McDermott, A. E. *J. Magn. Reson.* **2003**, *164*, 270−285.
(38) Maricq, M. M.; Waugh, J. S. *J. Chem. Phys.* **1979**, *70*, 3300−3316.
(39) Tjandra, N.; Szabo, A.; Bax, A. *J. Am. Chem. Soc.* **1996**, *118*, 6986−6991.
(40) Reif, B.; Hennig, M.; Griesinger, C. *Science* **1997**, *276*, 1230−1233.

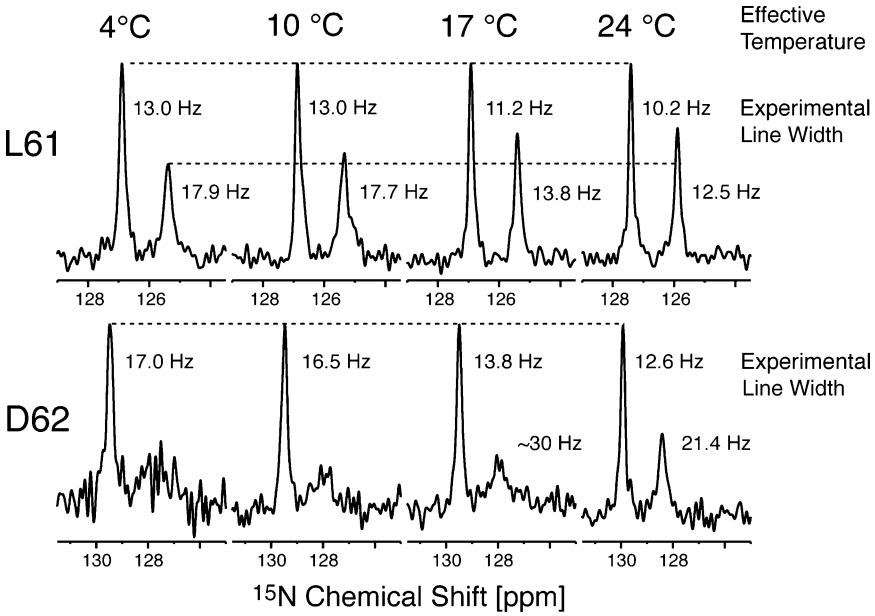

Figure 3. 1D columns along the ^{15}N dimension in a ^{1}H coupled ^{1}H,^{15}N correlation experiment in the solid state for different temperatures. The MAS frequency was set to 13 kHz. The effective temperature, as well as the line width (FWHM) of each resonance, is indicated in the figure. Only at increased temperatures the upfield component for the correlation signal of the amid of D62 is visible in the spectrum. Spectra recorded at all temperatures are reproduced after multiple heating and cooling cycles.

motion, the spectral density function $J(\omega)$ is given as $J(\omega) = \tau_C/(1 + \omega^2\tau_C^2)$. In addition to the size and relative orientation of the CSA and dipolar tensors, the cross-correlated relaxation rate is therefore directly proportional to the size of the molecular correlation time τ_C. Assuming that the protein backbone is significantly dynamic in the solid state, the ratio of the ^{15}N−H$^{\alpha}$/H$^{\beta}$ multiplet intensities will be affected. In the solid state, the exact size of the expected effect for an individual amide site is governed by the corresponding spectral density function implicated in the underlying motional model. It is important to note that motions occurring on time scales which are fast compared to the rotor revolution will not depend on the MAS rotation frequency.

In general, we observe larger effects for ^{15}N compared to ^{1}H. We speculate that the limited resolution in the ^{1}H dimension is due to residual ^{1}H,^{1}H dipolar couplings despite the very high deuteration levels employed in this study. This is corroborated by the MAS spinning frequency dependence of the ^{1}H line width as reported earlier.[22] In the following, we focus therefore on the analysis of cross-correlated relaxation in the ^{15}N dimension. We expect that, with future availability of higher MAS rotation frequencies (>30 kHz), the effects, described now for ^{15}N, will become observable for ^{1}H.

In order to identify motional properties as the source of the effect, we recorded temperature dependent ^{1}H,^{15}N correlation spectra without ^{1}H decoupling in the indirect ^{15}N dimension.

Figure 3 represents the ^{15}N dimension of a ^{1}H coupled ^{1}H,^{15}N correlation experiment for correlation signals resulting from the amide moiety of L61 and D62 recorded at different temperatures. Clearly, the experimental differential NH$^{\alpha}$/NH$^{\beta}$ intensity is temperature dependent. Since all experimental parameters which influence static properties (like, e.g., the MAS frequency and angle) are kept constant, we conclude that only local dynamics can be responsible for this effect. In addition, we observe variations in the relaxation behavior for different residues in the protein indicating that indeed local motional effects are detected.

The upfield component of D62 is broadened beyond detection in the ^{15}N dimension for temperartures below 17 °C. This residue therefore constitutes a typical case for which TROSY type techniques should be beneficial in order to increase the resolution and sensitivity in the NMR spectra. The size of the line width of the ^{1}H scalar decoupled ^{1}H,^{15}N correlation spectrum adopts approximately the average line width of the upfield and downfield components (Figure 4). If we select only the narrow component of the spectrum, the apparent resolution in the ^{15}N dimension can be increased. This can be achieved by application of spin state selective excitation (S3E) techniques.[43] Spin state selective experiments have recently been successfully applied in the solid state in order to achieve homonuclear scalar decoupling in uniformly ^{13}C enriched peptides and proteins.[44] In particular, we recorded an IPAP ^{1}H,^{15}N correlation experiment[45,46] in which in-phase and anti-phase correlation signals are added and subtracted in order to yield only the upfield or downfield component of the doublet. Details on the experimental setup are included in the Supporting Information. Smaller but still significant effects are observed, if the temperature of the sample is raised to 24 °C. Our experiments show that the ^{15}N line width can be strongly affected by backbone motion induced by moderate temperature changes. The dynamic properties of other biomolecules, like membrane proteins and fibrillar aggregates, are likely to be different but might result in undetectable broadening of the ^{15}N

(41) Chekmenev, E. Y.; Zhang, Q.; Waddell, K. W.; Mashuta, M. S.; Wittebort, R. J. *J. Am. Chem. Soc.* **2004**, *126*, 379−384.
(42) Wylie, B. J.; Franks, W. T.; Rienstra, C. M. *J. Phys. Chem. B* **2006**, *110* (22), 10926−10936.
(43) Sorensen, M. D.; Meissner, A.; Sorensen, O. W. *J. Magn. Reson.* **1999**, *137* (1), 237−242.
(44) Duma, L.; Hediger, S.; Brutscher, B.; Böckmann, A.; Emsley, L. *J. Am. Chem. Soc.* **2003**, *125*, 11816−11817.
(45) Ottiger, M.; Delaglio, F.; Bax, A. *J. Magn. Reson.* **1998**, *131*, 373−378.
(46) Andersson, P.; Weigelt, J.; Otting, G. *J. Biomol. NMR* **1998**, *12* (3), 435−441.

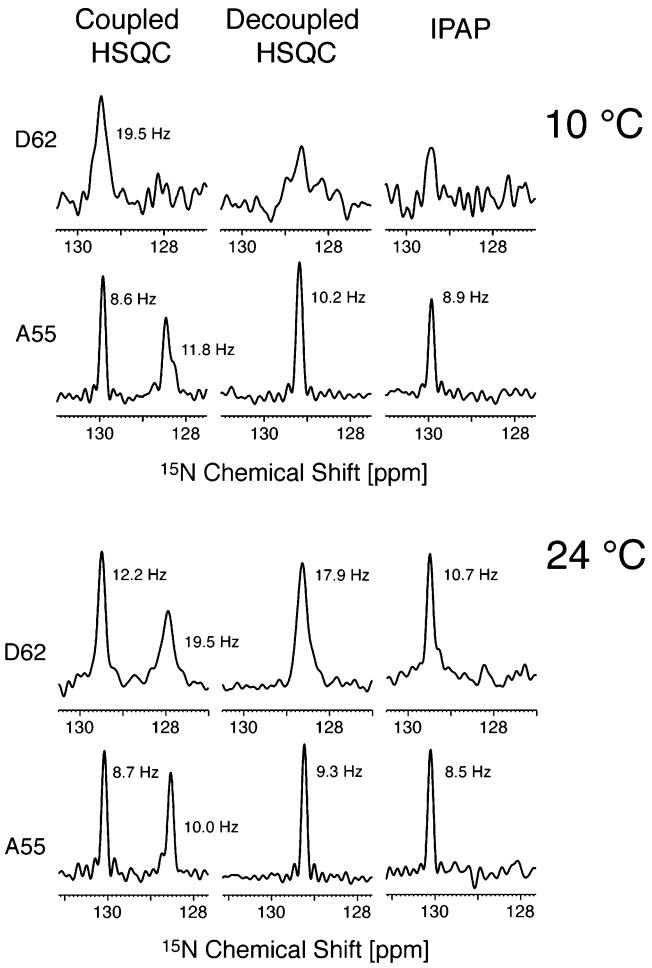

Figure 4. 1D columns along the ^{15}N dimension in ^{1}H,^{15}N correlation experiments (HSQC: Heteronuclear Single Quantum Correlation; IPAP: *I*n-*P*hase *A*nti-*P*hase) in the solid state. For the spectra shown at the top and the bottom of the figure, the effective temperature was set to 10 and 24 °C, respectively. The MAS frequency was adjusted to 24 kHz in both cases. The line width (FWHM) of each resonance is indicated in the figure. Experimental details on the employed pulse sequences are provided as part of the Supporting Information.

resonances if standard solid-state NMR experiments are employed. The effective resolution can then only be increased by application of TROSY type techniques on highly deuterated biomolecules.

In order to quantify the motional contribution to the intensities, we determined the differential ^{15}NH$^{\alpha/\beta}$ multiplet intensities as a function of the MAS frequency. Equation 2 summarizes the above-mentioned effects which contribute to the ratio of the ^{15}NH$^{\alpha/\beta}$ multiplet intensities

$$\frac{I(\mathrm{NH}^{\beta})}{I(\mathrm{NH}^{\alpha})} = 1 + A(\delta_N,\beta^{N,\mathrm{NH}})\,\tau_R^X + \mathrm{B}(\beta^{RL})\,\tau_R^Y + C(\tau_C) \quad (2)$$

The prefactor A comprises all terms related to the static values of the CSA anisotropy δ_N as well as the ^{1}H−^{15}N dipole and the angle β between the principal axes of the two anisotropies. It can be shown that the differential intensity is independent of the asymmetry parameter η of the ^{15}N CSA (see Supporting Information). B is a correction term which takes into account a possible misadjustment of the magic angle. C describes the dynamic contribution and is independent of the MAS rotation frequency. Equation 2 is a purely heurisitic equation. Therefore,

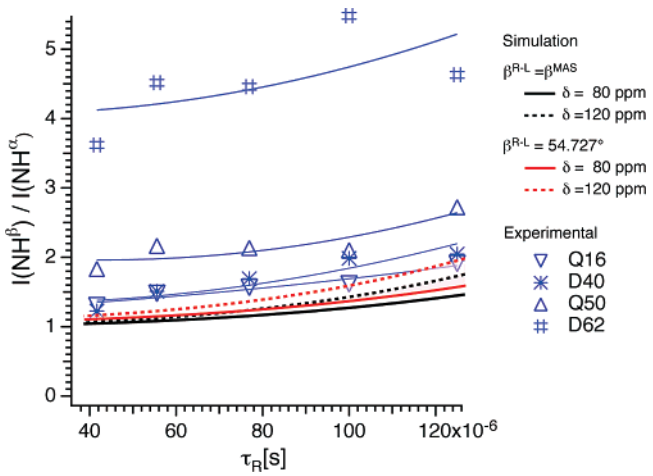

Figure 5. Experimental (blue symbols) and simulated ratio of the ^{15}NH$^{\alpha/\beta}$ multiplet intensities as a function of the MAS rotor period τ_R. Red and black lines are based on simulations using the program SIMPSON.[47] Variation of the reduced anisotropy δ_z results in ^{15}NH$^{\alpha/\beta}$ multiplet intensity ratios which are within the gray or red shaded area, respectively. Missetting of the magic angle (resulting in a differential line width of 1 Hz) is indicated as a red line ($\beta^{MA} = \beta^{RL} = \arctan(\sqrt{2}) \approx 54.735\,61$). In all simulations, the angle between the principal axes of the dipolar and the CSA interaction tensors was assumed to be 20°. Obviously, motional effects result in a constant offset of the NH$^{\alpha/\beta}$ intensity ratio independent of the MAS rotation frequency (represented as blue line, e.g., for the residue D62). Blue lines are included in order to guide the eye and are not based on simulations. Heating effects induced by friction due to MAS are accounted for in all experiments by adjusting the temperature so that the HDO resonance adopts a chemical shift corresponding to 10 °C. Spectra were recorded at an external magnetic field strength of $B_0 = 14.1$ T.

the dimensionalities on the left-hand and right-hand side of the equation must not necessarily match. A, B, X, and Y are in the following determined by simulations using the program SIMPSON developed by Nielsen and co-workers.[47] In the simulations, we calculated the NH$^{\beta}$/NH$^{\alpha}$ relative intensities as a function of the MAS spinning frequency. The simulations were performed assuming different values for the reduced ^{15}N CSA (solid and dashed black lines in Figure 5). In the first set of simulations, it is assumed that the magic angle is set correctly. Therefore, B is set to zero. Assuming no motion ($C = 0$), the parameters A and X in eq 2 are obtained by a least-squares fit of the simulated intensity ratios $I(\mathrm{NH}^{\beta})/I(\mathrm{NH}^{\alpha})$. We can fit $X = 2.4$, and $A = 9.3 \times 10^8$ and 2.6×10^9 for a ^{15}N chemical shift anisotropy of 80 and 120 ppm, respectively.

To appreciate the effect of magic angle miscalibration, we performed a second set of simulations in which the angle between the rotor axis and the external magnetic field was set to 54.727° (which is approximately 0.009° off from the magic angle) (solid and dashed red lines in Figure 5). Again, assuming no motion ($C = 0$), the least-squares fit of the simulated data showed that the magic angle miscalibration induces an offset to the ratio of the ^{15}NH$^{\alpha/\beta}$ multiplet intensities (with $Y \approx 0$, $B = 0.08$, A and X as above). At the same time, this particular missetting of the magic angle causes a 1 Hz difference in the line width of the ^{15}NH$^{\alpha/\beta}$ multiplet components. This is the approximate minimum differential line width that we observe at high temperatures and fast spinning (24 kHz). Even assuming this relatively large deviation from the ideal condition, our experimental data deviate significantly from the simulated

(47) Bak, M.; Rasmussen, J. T.; Nielsen, N. C. *J. Magn. Reson.* **2000**, *147*, 296−330.

curves. We can therefore exclude miscalibration of the magic angle as a potential source of the observed effect. In addition, magic angle mis-setting would yield the same effect on the multiplet intensities for all residues in the protein. We observe, however, large variations for different amino acids.

Solid blue lines in the figure were included in order to guide the eye and are not the result of simulations. Figure 5 summarizes simulations and experimental data for selected residues. Care was taken to compensate for heating effects due to sample spinning. We find that MAS sample spinning induces a temperature increase which is caused by friction (see Supporing Information, S5). Due to activation of motion, a temperature increase results in a differential NH^{α}/NH^{β} intensity ratio (Figure 3). To guarantee a constant temperature within the sample for the MAS dependent analysis of the NH differential intensities, we adjusted the set temperature on the temperature control unit such that the water resonance appears at the same chemical shift in all experiments.

In conclusion, we have shown that dynamics in the nanosecond−microsecond time scale can indeed induce significant line broadening of ^{15}N resonances in solid-state NMR. Averaging of $^{15}N-H^{\alpha/\beta}$ multiplet components due to ^{1}H decoupling induces an effective relaxation of the ^{15}N coherence. In the absence of static conformational heterogeneity, high resolution solid-state NMR spectra can only be recorded by application of TROSY type techniques which select the narrow component of the multiplet pattern. We speculate that this effect has been obstructing the NMR spectroscopic characterization of many membrane proteins and fibrillar aggregates. Only in very favorable cases, in which dynamics are of either very small amplitude or very fast (picosecond), can high-resolution spectra be obtained. We expect that this approach, which requires high levels of deuteration, will have a significant impact on the quality of solid-state NMR spectroscopic investigations in the future.

Materials and Methods

Sample Preparation. A pET3d derivative coding for α-spectrin SH3 domain from chicken brain was a gift of M. Saraste. Protein was expressed in *E. coli* BL21 (DE3) in M9 minimal medium with 100% D_2O with 4 g/L $^{2}H_8$-glycerol as the sole carbon source, together with 1 g/L $^{15}N-NH_4Cl$. Cells were grown at 37 °C up to an optical density (OD_{600nm}) of 0.6. The temperature was then decreased to 22 °C, and induction was started with 1 mM IPTG overnight. Purification of the cell extract was carried out in H_2O containing buffer systems as reported earlier (anion exchange on a Q-Sepharose FF column, followed by gel filtration on a Superdex75 column).[48] This yields an amide protonated, carbon deuterated preparation. 5 mg of that sample were lyophilized and redissolved in H_2O/D_2O using a mixing ratio of 10:90 with respect to solvent exchangeable protons. Microcrystalline precipitates were obtained by mixing the protein solution (10 mg/mL) at a ratio of 1:1 with a 200 mM $(NH_4)_2SO_4$ solution (in H_2O 90% D_2O; the pH value was adjusted to around 7 using an alkaline atmosphere).

NMR Spectroscopy. MAS solid-state NMR experiments were performed at a magnetic field strength of 14.1 T, employing a Bruker Avance 600WB spectrometer. The spectrometer was equipped with a standard 3.2 mm triple resonance MAS probe. $^{1}H,^{15}N$ correlations were acquired using the pulse sequence described previously,[22] omitting decoupling in either the direct and/or indirect evolution period to yield scalar coupled multiplets. In order to achieve spin state selection in the ^{15}N dimension, we employed the IPAP scheme introduced originally by Bax, Otting and co-workers.[45,46] All employed pulse sequences are described in detail in the Supporting Infomation.

Acknowledgment. We thank Dr. Uwe Müller, BESSY, Berlin, for assistance in collecting the X-ray data. This research was supported by the DFG Grant Re1435. The authors thank Prof. Hartmut Oschkinat for continuous support of this project.

Supporting Information Available: Considerations on the ^{15}N-CSA and $^{1}H,^{15}N$ dipole interference in the static case; definition of the employed CSA convention; investigation of Magic Angle Missetting on the $^{15}N-H^{\alpha}/^{15}N-H^{\beta}$ multiplet pattern; effects of variations of the size and orientation of the ^{15}N CSA tensor on the $^{15}N-H^{\alpha}/^{15}N-H^{\beta}$ differential multiplet intensities; Sample heating due to friction induced by sample spinning; NMR pulse sequences. This material is available free of charge from the Internet via the Internet at http://pubs.acs.org.

JA072024C

(48) Pauli, J.; Van Rossum, B.-J.; Förster, H.; De Groot, H. J. M.; Oschkinat, H. *J. Magn. Reson.* **2000**, *143*, 411−416.